THE JOURNAL OF BIOLOGICAL CHEMISTRY VOL. 290, NO. 7, pp. 4512–4527, February 13, 2015

Synaptic Synthesis, Dephosphorylation, and Degradation

*A NOVEL PARADIGM FOR AN ACTIVITY-DEPENDENT NEURONAL CONTROL OF CDKL5**

Received for publication, June 17, 2014, and in revised form, December 19, 2014 Published, JBC Papers in Press, January 2, 2014, DOI 10.1074/jbc.M114.589762

Paolo La Montanara[‡], Laura Rusconi[‡], Albina Locarno[‡], Lia Forti[‡], Isabella Barbiero[‡], Marco Tramarin[‡], Chetan Chandola[‡], Charlotte Kilstrup-Nielsen[‡1], and Nicoletta Landsberger[‡§1,2]

From the [‡]Department of Theoretical and Applied Sciences, Section of Biomedical Research; University of Insubria, 21052 Busto Arsizio, Italy and the [§]San Raffaele Rett Research Unit, Division of Neuroscience, San Raffaele Scientific Institute, 20132 Milan, Italy

Background: Although associated with intellectual disability, CDKL5 functions and regulation are poorly understood.
Results: Upon neuronal activation, CDKL5 is dynamically regulated through local synthesis, dephosphorylation, and degradation.
Conclusion: Neuronal activity and maturation control CDKL5 phosphorylation state and expression.
Significance: This is the first report showing the activity-dependent modulation of CDKL5 in the neuronal periphery, further linking it to synapse development and plasticity.

Mutations in the X-linked *CDKL5* (cyclin-dependent kinase-like 5) gene have been associated with several forms of neurodevelopmental disorders, including atypical Rett syndrome, autism spectrum disorders, and early infantile epileptic encephalopathy. Accordingly, loss of CDKL5 in mice results in autistic-like features and impaired neuronal communication. Although the biological functions of CDKL5 remain largely unknown, recent pieces of evidence suggest that CDKL5 is involved in neuronal plasticity. Herein, we show that, at all stages of development, neuronal depolarization induces a rapid increase in CDKL5 levels, mostly mediated by extrasomatic synthesis. In young neurons, this induction is prolonged, whereas in more mature neurons, NMDA receptor stimulation induces a protein phosphatase 1-dependent dephosphorylation of CDKL5 that is mandatory for its proteasome-dependent degradation. As a corollary, neuronal activity leads to a prolonged induction of CDKL5 levels in immature neurons but to a short lasting increase of the kinase in mature neurons. Recent results demonstrate that many genes associated with autism spectrum disorders are crucial components of the activity-dependent signaling networks regulating the composition, shape, and strength of the synapse. Thus, we speculate that CDKL5 deficiency disrupts activity-dependent signaling and the consequent synapse development, maturation, and refinement.

CDKL5 (cyclin-dependent kinase like 5)[3] is an X-linked gene that has been associated with early onset epileptic encephalopathies characterized by the onset of intractable epilepsy within the first weeks of life, severe developmental delay, hypotonia, and some Rett syndrome-like features (1). *CDKL5* encodes a serine/threonine kinase that is characterized by an N-terminal catalytic domain and a long C-terminal tail regulating the catalytic activity, subcellular localization, and stability of the protein (2, 3). In human and mouse, the *CDKL5*/*Cdkl5* mRNA and protein are widely expressed with a well recognized enrichment in brain (4). In mouse brains, CDKL5 is weakly expressed during embryogenesis and gets markedly up-regulated during postnatal development (3, 4); furthermore, *Cdkl5* transcription is regulated by various stimuli, depending on the specific brain district. Indeed, cocaine treatment of rats significantly reduces *Cdkl5* mRNA levels in the striatum but not in the frontal cortex (5). At the cellular level, CDKL5 is easily detectable in all neuronal compartments, including the nucleus, cytoplasm, and postsynaptic fraction (6). Loss of function studies have demonstrated that CDKL5 is required for neurite outgrowth, dendritic spine development, and excitatory synapse stability (4, 6, 7). The first *Cdkl5* knock-out mouse model is characterized by motor, social, and anxiety deficits similar to those observed in other autism and Rett syndrome mouse models; *Cdkl5*-null mice display also impaired learning and memory and altered event-related potentials (8, 9). Deficits were also found in neural circuit communication and in multiple signaling pathways, including that of AKT-mammalian target of rapamycin (mTOR), already linked to MeCP2 and Rett syndrome (10).

Neuronal activity is known to influence dendritic outgrowth, synaptic maturation, and plasticity. In particular, membrane depolarization and the subsequent calcium influx trigger a variety of cellular changes, including post-translational modification of synaptic molecules, the induction of localized protein synthesis within dendrites and gene transcription in the nucleus. Altogether, these events regulate synaptic function and the response of neuronal circuits to experience (11). These neuronal activity-dependent mechanisms are involved in learn-

* This work was supported by Telethon Grant GGP10032, Ministero della Salute (Ricerca Finalizzata 2008, Bando Malattie Rare) and the Jerome Lejeune Foundation and Cariplo Grant 2010-0724 (to N. L.) and by DisChrom Grant 238242, IRSF/IFCR (International Rett Syndrome Foundation/International Foundation for CDKL5 Research), and the Jerome Lejeune Foundation (to C. K. N.).

[1] These authors contributed equally to this work.
[2] To whom correspondence should be addressed: Dept. of Theoretical and Applied Sciences, Section of Biomedical Research, University of Insubria, Via Manara 7, 21052 Busto Arsizio, Italy. Tel.: 39-0331339406; E-mail: landsben@uninsubria.it.

[3] The abbreviations used are: CDKL5, cyclin-dependent kinase-like 5; AMPAR, α-amino-3-hydroxy-5-methyl-4-isoxazolepropionic acid receptor; *AP5*, (2*R*)-amino-5-phosphonovaleric acid; CNQX, 6-cyano-7-nitroquinoxaline-2,3-dione; NMDAR, NMDA receptor; PSD-95, postsynaptic density 95; PP1, protein phosphatase 1; DIV, days *in vitro*; N2a, Neuro 2a; P*n*, postnatal day *n*; WB, Western blotting; OA, okadaic acid; CaMK, calmodulin kinase.

ing and memory and adaptive behavioral responses; accordingly, autism spectrum disorders have often been associated with crucial components of the activity-dependent signaling networks regulating synaptic maturation and function (12). Considering that CDKL5 (i) is associated with autism spectrum disorders; (ii) is required for learning and memory and neuronal maturation; (iii) gets transiently phosphorylated upon BDNF stimulation (4); and (iv) gets excluded from the nucleus upon extrasynaptic NMDA receptors (NMDAR) activation (13), we hypothesized that it might be involved in activity-dependent signaling networks. We therefore investigated how neuronal activity regulates CDKL5, at both transcriptional and post-transcriptional levels.

Herein, we show that neuronal depolarization induces CDKL5 within 5 min through NMDARs and mainly relying on local protein synthesis. The increase of CDKL5 is transient and is rapidly followed in mature neurons by its proteasomal degradation. We suggest that this response depends on changes in the phosphorylation state of CDKL5 and requires the activation of NMDARs and protein phosphatase 1 (PP1). Indeed, only in neurons beyond a critical developmental stage, NMDAR activation induces the dephosphorylation of CDKL5, prompting its degradation. Eventually, *Cdkl5* transcription is activated, although with slower kinetics, resembling those of immediate early genes. We speculate that the kinase might be a crucial component of activity-dependent signaling pathways and, therefore, might affect synapse development and plasticity.

EXPERIMENTAL PROCEDURES

Mice—Mice (CD1 genetic background) were housed and treated according to the regulations on mouse welfare and ethics and with the approval of the institutional animal care and use committee of the University of Insubria.

Antibodies—The following antibodies were used for Western blotting and immunofluorescence experiments: rabbit polyclonal anti-CDKL5 (Sigma Prestige HPA002847) (6), anti-CaMKIIα (Abcam, ab92332), anti-phospho-CaMKIIα (T286, Abcam, ab124880), polyclonal rabbit anti-ERK1/2 (Millipore, 06-182), rabbit polyclonal anti-phospho-p44/42 ERK (Thr-202/Tyr-204; Cell Signaling, 9101), mouse monoclonal anti-CREB (Cell Signaling, 9104), mouse monoclonal anti-phospho-CREB (S133; Cell Signaling, 9196), mouse monoclonal anti-neuronal class III-β-tubulin (clone Tuj1; Covance, MMS-435P), mouse monoclonal anti-MAP2 (Millipore, anti-MAP2 clone AP20), rabbit polyclonal anti-PSD-95 (Cell Signaling, 2507), rabbit monoclonal anti-synapsin 1 (Cell Signaling, D12G5), mouse monoclonal anti-synaptophysin 1 (Synaptic Systems, 101011), and rabbit polyclonal anti-H3 (Abcam, ab1791). HRP-conjugated goat anti-mouse or anti-rabbit secondary antibodies for Western blotting were purchased from Thermo Scientific.

Primary Neuronal Cultures and Cell Lines—Primary cortical and hippocampal cultures were prepared from brains of CD1 mouse embryos at 17 days, considering the day of the vaginal plug as embryonic day 0, as described previously (3), and plated on poly-L-lysine-coated dishes at different densities (hippocampal neurons, 16,000 cells/cm^2; cortical neurons, 26,000 cells/cm^2). After 4 days *in vitro* (DIV4), cytosine-1-β-D-arabinofuranoside (Sigma-Aldrich) was added at the final concentration of 2 μM to prevent astroglial proliferation. The murine neuroblastoma cells, Neuro 2a (N2a), were grown in MEM supplemented with 10% fetal bovine serum, penicillin (100 IU/ml), and streptomycin (100 μg/ml) at 37 °C in a humidified 5% CO_2 atmosphere.

Treatment of Cultured Cells—Neurons were treated at DIV3, 7, 14–16, and 21 as indicated in the text for 5 min with 50 mM KCl in KRH (85 mM NaCl, 1.2 mM KH_2PO_4, 1.2 mM $MgSO_4$, 2 mM $CaCl_2$, 25 mM Hepes, pH 7.5, 1.1 mg/ml glucose). Control cells were incubated in KRH containing 5 mM KCl and 130 mM NaCl. Longer KCl treatments were performed adding 50 mM KCl (or 50 mM NaCl to controls, thus maintaining the osmotic concentration of monovalent cations) directly to the medium. Moreover, when indicated, KCl-dependent depolarization was preceded by incubation with EGTA (2 mM, 20 min), U0126 (10 μM, 20 min; Promega), (AP5; 100 μM, 30 min; Sigma-Aldrich), CNQX (6-cyano-7-nitroquinoxaline-2,3-dione disodium salt; 40 μM, 30 min; Sigma-Aldrich), cycloheximide (40 μM; 30 min; Sigma-Aldrich), MG132 (50 μM; 3 h; Sigma-Aldrich), and actinomycin D (20 μg/ml; 30 min; Sigma-Aldrich). As phosphatase inhibitors we used okadaic acid (1 μM or 20 nM; 45 min; Sigma-Aldrich), Na_3VO_4 (1 mM, 1 h; Sigma-Aldrich), calyculin (100 nM; 45 min; Sigma-Aldrich), and deltamethrin (20 nM; 45 min; Sigma-Aldrich). The efficacy of the phosphatase inhibitors was verified by Western blotting using antibodies against phosphotyrosine (Cell Signaling, 9411) and phosphoserine/phosphothreonine (BD Biosciences, 612548), respectively. Neurons were also exposed to the following activators: forskolin (100 μM; 5 min; Sigma-Aldrich), NMDA (50 μM; 5 min; Sigma-Aldrich), and BDNF (50 μg/ml; Pepro Tech; 450-02). Neurons were lysed in Laemmli buffer and processed for immunoblotting.

Preparation and Treatment of Cortical Slices—CD1 mice (P2.5–P35) were anesthetized with halothane (Sigma-Aldrich) and decapitated. The brain was quickly removed and put in ice-cold cutting solution (125 mM NaCl, 2.5 mM KCl, 1.25 mM NaH_2PO_4, 26 mM $NaHCO_3$, 10 mM D-glucose, 2 mM $CaCl_2$, 1 mM $MgCl_2$) saturated with 95% oxygen and 5% CO_2 (pH 7.4). Cortical-subcortical coronal frontal slices (anteriorly to the lateral ventricles) were then cut at a thickness of 200 μm with a Leica VT1000S vibratome and maintained at 32 °C for 30 min to allow functional recovery and later kept at 25 °C in the same buffer. Recovered slices were transferred in a perfusion chamber and perfused (1 ml/min) at room temperature for 5 min, 20 min, or 1 h with a gassed (95% 0_2/5% CO_2) solution (1.25 mM KH_2PO_4, 1.3 mM $MgSO_4$, 2.5 mM $CaCl_2$, 17.6 mM $NaHCO_3$, 10 mM D-glucose, pH 7.4) containing isomolar low or high [K^+] (125 mM NaCl, 3 mM KCl or 98 mM NaCl, 30 mM KCl, respectively) in accordance with a previously published protocol (14). After perfusion, the slides were rapidly lysed in a potter with 200 μl of lysis buffer (50 mM Tris-HCl, pH 7.4, 150 mM NaCl, 1% Triton X-100, 2 mM EDTA, 1 mM DTT, 1 mM PMSF, 1 mM NaF, 1 mM Na_3VO_4, phosphatase inhibitor mixture (Roche), and protease inhibitor mixture (Sigma)). The protein content of the samples was measured using the Bio-Rad Bradford method, and the samples were processed by immunoblotting.

Electrophysiology—Whole cell voltage or current clamp recordings were obtained from cultured hippocampal neurons

at DIV7–DIV19 using a Multiclamp 200B amplifier. Current/voltage traces were filtered at 2 KHz and acquired at 10 KHz with a Digidata 1440A interface. During recordings, cells were bathed in standard bicarbonate-buffered external saline (125 mM NaCl, 2.5 mM KCl, 1.25 mM NaH_2PO_4, 26 mM $NaHCO_3$, 2 mM $CaCl_2$, 1 mM $MgCl_2$, 10 mM glucose, pH 7.4, after saturation with 5% CO_2, 95% O_2) at room temperature. For high K^+ stimulation, a modified external saline was obtained from bicarbonate-buffered external saline by decreasing NaCl to 78.5 mM and increasing KCl to 50 mM. All solutions were bath-applied at 2 ml/min. Patch pipettes (3–5 MOhm final resistance) were filled with a potassium gluconate-based internal solution (145 mM potassium gluconate, 6 mM NaCl, 0.2 mM EGTA, 1 mM $MgCl_2$, 4 mM ATP-Mg, 0.4 mM GTP-Na_2, pH 7.35).

Propidium Iodide Staining—Cortical slices (100 μm) of mouse brains at different ages were perfused with a gassed (95% 0_2/5% CO_2) solution (1.25 mM KH_2PO_4, 1.3 mM $MgSO_4$, 2.5 mM $CaCl_2$, 17.6 mM $NaHCO_3$, 10 mM D-glucose, pH 7.4) containing isomolar low or high [K^+] (125 mM NaCl, 3 mM KCl or 98 mM NaCl, 30 mM KCl, respectively) for 1 h or to induce necrosis with 0.5 mM Cd^{2+} for 3 h and subsequently incubated with 2.5 μg/ml propidium iodide in KRH (130 mM NaCl, 5 mM KCl, 1.2 mM KH_2PO_4, 1.2 mM $MgSO_4$, 2 mM $CaCl_2$, 25 mM Hepes, pH 7.5, 1.1 mg/ml glucose) for 15 min on ice. After two washes the slices were fixed in 4% paraformaldehyde for 1 h on ice, washed twice with PBS, dehydrated, and mounted for microscopy analysis. The images were taken at a Nikon Eclipse Ni microscope equipped with a Nikon Digital Sight DS-2MBWc camera with fixed exposure time.

Cultured hippocampal neurons were treated with KCl for 5 min or 3 h or, as controls for cell death, with 0.5 mM Cd^{2+} or 200 μM H_2O_2 for 3 h and washed with ice-cold KRH solution. Subsequently, neurons were incubated for 15 min with 2.5 μg/ml propidium iodide in KRH on ice, washed twice, and fixed with 4% paraformaldehyde. Fixed neurons were immunostained with anti-synapsin 1 and counterstained with DAPI. Images were taken with an IN Cell Analyzer 1000 at the ALEMBIC facility (San Raffaele Scientific Institute, Milan, Italy), and the percentage of propidium iodide positive neurons with respect to the total number of neurons (synapsin 1 positive) was calculated. For each time point, an average of 150 cells were analyzed.

Apoptosis Assays—TUNEL stain was used to analyze the presence of apoptosis in cortical slices (100 μm) perfused with 30 mM KCl (1 h) as described above or as a control with 0.5 mM Cd^{2+} (3 h). The slices were fixed with 4% paraformaldehyde as above, and the NeuroTACS™ II *in situ* apoptosis detection kit (Trevigen) was used following the manufacturer's instructions. Images were taken with an Axio ImagerA2 equipped with an AxioCam MRm camera (Zeiss), keeping a fixed exposure time.

Somatodendritic Fractionations—High density cortical neurons (100,000/cm^2) at DIV16 were treated for 5 min with 50 mM KCl (or as control with 50 mM NaCl) at 37 °C, rinsed with Hanks' balanced salt solution, and treated for 2 min with papain (0.1 mg/ml; Sigma-Aldrich) and DNase (50 μg/ml; Sigma-Aldrich) in Hanks' balanced salt solution at 37 °C. In some experiments, MG132 (50 μM) was included to avoid protein degradation. The cultures were then rinsed three times with ice-cold PBS and covered with 1.5 ml/dish (60 mm) of an ice-cold buffer (10 mM Tris-HCl, pH 7.4, 150 mM NaCl, 0.5 mM EGTA, protein inhibitor cocktail, 1 mM NaF, 1 mM $NaVO_4$, 1 mM PMSF, 0.5 mM DTT) containing 0.35 M sucrose, transposed to a new tube, and then mixed 1:1 with a similar solution containing 0.8 M sucrose. The final solution was then passed through a plastic wide tip to break down the neuronal network. The nuclear-somatic pellet was isolated after centrifugation at 1500 × *g* for 10 min at 4 °C, whereas the supernatant was further centrifuged at 28,000 × *g* for 10 min, producing the dendritic pellet enriched in pre- and postsynaptic structures. At the end the pellets were resuspended in lysis buffer (50 mM Tris-HCl, pH 7.4, 150 mM NaCl, Nonidet P-40 1%, 1 mM EDTA, 0.5 mM DTT, protein inhibitor cocktail, 1 mM PMSF) and analyzed by WB.

Synaptoneurosome Preparation—Synaptoneurosomes were prepared mainly as described in De Rubeis *et al.* (15): cortices from young adult (P30–P35) female mice (CD1) were homogenized in 1 ml of homogenization buffer (0.32 M sucrose, 0.1 mM $CaCl_2$, 1 mM $MgCl_2$, 0.1 mM PMSF) in ice using a Teflon glass homogenizer. The homogenate was brought to a final sucrose concentration of 1.25 M by adding 4.66 ml of 2 M sucrose and 2 ml of 0.1 mM $CaCl_2$ solution where after the sample was loaded into the centrifuge tubes and overlaid first with an equal volume of 1.0 M sucrose, 0.1 mM $CaCl_2$ solution and thereafter with the homogenization buffer. The samples were centrifuged at 100,000 rpm for 3 h at 4 °C (Beckman TLA 100.4). The pellet corresponding to the somatic/nuclear fraction was resuspended in 1 ml of resuspension buffer (20 mM Hepes, pH 7.4, 147 mM NaCl, 3 mM KCl, 10 mM glucose, 2 mM $MgSO_4$, 2 mM $CaCl_2$), whereas the synaptoneurosomes were recovered in the interphase of the 1.25 M/1 M sucrose fractions and pelleted by centrifugation at 15,000 × *g* for 10 min at 4 °C and finally resuspended in 1 ml of resuspension buffer. The synaptoneurosomes were equilibrated by incubation at 37 °C for 30 min before stimulation with 50 mM KCl for 5 min at 37 °C; an isomolar exposition to NaCl was used as control. In the end, the synaptoneurosomes and the somatic/nuclear fraction were analyzed by Western blotting.

Immunofluorescence—Hippocampal neurons were processed for immunofluorescence as previously described (3). Images were taken with a Nikon Eclipse Ni microscope equipped with a Nikon Digital Sight DS-2MBWc camera. For the quantification of CDKL5 induction in dendrites, images were taken with a Leica TCS SP2 confocal microscope (ALEMBIC, San Raffaele Scientific Institute). Image analysis was performed with ImageJ software: the MAP2 signal was used to select the dendritic profile excluding the soma, and the corresponding CDKL5 fluorescence intensity was quantified.

Western Blot Analysis—Approximately 10 μg of protein extracts were heated (at 70 °C to preserve phosphorylation, otherwise at 95 °C) and separated by 8% SDS-PAGE (37.5:1 acrylamide:bis-acrylamide) using Tuj1 as internal standard. To enhance the separation of phosphorylated and nonphosphorylated CDKL5 isoforms, we exploited 7% SDS-PAGE with 77:1 acrylamide:bis-acrylamide. Filters were developed using Super-Signal West Pico Chemiluminescent Substrate (Pierce) or ECL Prime Western blotting detection reagent (GE Healthcare) and

quantified with a CCD camera (Syngene, G-Box Chemi XRQ) where each sample was measured relative to the background or by scanning densitometry using the QuantityOne software package (Bio-Rad). To evaluate the phosphorylation status, a ratio between the normalized phospho-protein and the normalized total isoforms of the same protein was calculated.

In Vitro Dephosphorylation Assay—Hippocampal DIV7 neurons were collected directly in lysis buffer (50 mM Tris-HCl, pH 8, 1 mM EDTA, 150 mM NaCl, 0.5 mM DTT, SDS 0,1%, protein inhibitor cocktail, 1 mM PMSF, Nonidet P-40 1%) with or without phosphatase inhibitors (1 mM NaF, 1 mM $NaVO_4$, phosphatase inhibitor mixture (Roche)). The protein extract was incubated with or without 800 units of λ-phosphatase (New England BioLabs) in a phosphatase reaction buffer (50 mM Tris-HCl, 5 mM DTT, 0.1 mM EDTA, 0.01% Brij 35, pH 7.5), supplemented with 2 mM $MnCl_2$ for 3 h at 30 °C. The reactions were stopped by incubation at 65 °C for 15 min, and the samples were analyzed by immunoblotting.

RNA Isolation and Quantitative RT-PCR Analysis—Total RNA was isolated using the miRNeasy Kit (Qiagen) according to the manufacturer's instructions. Contaminating DNA was removed with RQ1 RNase-free DNase (Promega), and the obtained RNA was quantified with a Biotech Ultrospec 2000 UV-visible spectrophotometer, and its quality was assessed through agarose gel electrophoresis. cDNA was synthetized from 200 ng of RNA using the SuperScript II reverse transcriptase kit (Invitrogen) as indicated by the manufacturers. Quantitative real time PCR was performed with a Chromo 4™ detector real time PCR machine with GoTaq® quantitative PCR Master Mix (Promega). The quantitative RT-PCR was performed in 25 μl using 10 ng of cDNA and the following cycling parameters: 15 s at 95 °C, 30 s at 60 °C, and 30 s at 72 °C. Each independent sample was analyzed in triplicate from RNA collected from at least three independent neuronal cultures. All quantitative RT-PCR values were normalized to GAPDH. A melting curve was automatically generated for each sample and confirmed that a single amplicon was generated in each reaction.

Total RNA was extracted from the synaptoneurosomes and the nuclear-somatic fraction using the miRNeasy kit (Qiagen) according to the manufacturer's instructions. After retrotranscription, the presence of *Cdkl5* mRNA, along with those of *Mecp2* and *Bdnf* were analyzed by PCR. The PCRs were performed in 20 μl using 50 ng of cDNA and the following cycling parameters: *Cdkl5*, 35 cycles: 1 min at 95 °C, 30 s at 50 °C, 1.5 min at 72 °C; *Mecp2* mRNA, 35 cycles: 30 s at 94 °C, 30 s at 63 °C, 30 s at 72 °C; and *Bdnf* mRNA, 35 cycles: 30 s at 95 °C, 1 min at 60 °C, 1 min at 72 °C. The forward (F) and reverse (R) primers were: m*Cdkl5* F, 5′-TTCCCAGCTGTTAACCATCC; m*Cdkl5* R, 5′-AAGGAGACCGGTCCAAAAGT; c-*Fos* F, 5′-GGCAAAGTAGAGCAGCTATCTCCT; c-*Fos* R, 5′-TCAGCTCCCTCCTCCGATTC; m*Gapdh* F, 5′-AAGGTCGGTGTGAACGGATTTG; m*Gapdh* R, 5′-GCAGTGATGGCATGGACTGTG; m*Bdnf* F, 5′-AAGTCTGCATTACATTCCTCGA; m*Bdnf* R, 5′-TTATCAATTCACAATTAAAGCAGCAT; and m*MeCP2* F, 5′-CAGCTCCAACAGGATTCCAT; m*MeCP2* R, 5′-TTGTAGTGGCTCATGCTTGC.

Statistical Analysis—All values are expressed as the average of at least three different experiments ± S.E. The significance of results was evaluated by Student's *t* test, one-way analysis of variance-Dunnett, or two-way analysis of variance test (Bonferroni post hoc analysis), and statistical significance was established as $p < 0.05$.

RESULTS

Neuronal Activation Triggers a Rapid, Protein Synthesis-dependent Increase in CDKL5 Levels—As described in the introduction, CDKL5 might play a pivotal role in converting the effects of transient neuronal stimuli into changes in the molecular pathways that are important for the brain to process information. To analyze whether CDKL5 expression might be affected by neuronal membrane depolarization and in analogy with several studies based on long and short KCl treatments as a paradigm for neuronal activation (16, 17), we treated primary hippocampal neurons, prepared from embryonic day 17 mouse embryos and cultured for *in vitro* for 7 days, with KCl (50 mM) for 5 min. Neuronal activation was confirmed by WB, using phospho-specific antibodies against CaMKIIα (T286), CREB (S133), and ERK1/2 (Thr-202 and Tyr-204), respectively, with respect to total protein levels (Fig. 1*A*). Neuronal viability was assessed by current clamp or voltage clamp whole cell recordings in which the recovery of spiking activity during KCl-induced depolarization block was verified (Fig. 2, *A*–*C*) together with the presence of spontaneous postsynaptic potentials or currents with frequency similar to the control (Fig. 2*D*). As further controls, we used propidium iodide staining to verify that short or prolonged treatments with KCl are not toxic to neuronal cultures at different maturation stages (Fig. 2*E*).

The response of CDKL5 to neuronal depolarization was analyzed by using a specific antibody (6), and as shown in Fig. 1 (*B* and *C*), CDKL5 levels significantly increased after 5 min of treatment; as expected, no increment could be detected in the protein levels of ERK1/2 and c-Fos (Fig. 1*C* and data not shown). To confirm the KCl-dependent induction in an *ex vivo* model, cortical slices from young adult mice (P30–P35) were stimulated with KCl (30 mM) for 5 min. As shown in Fig. 1 (*D* and *E*), WB analyses confirmed that CDKL5 levels are promptly increased in response to membrane depolarization also in a complex neuronal network. As before, we controlled the toxicity of short and long term KCl treatments in brain slices of different developmental ages by analyzing cell mortality through propidium iodide staining and DNA fragmentation through TUNEL assays (Fig. 2, *F* and *G*, respectively).

We investigated whether the observed fast increase in CDKL5 protein levels was regulated at the transcriptional or translational level. Pretreatment of hippocampal neurons with the protein synthesis inhibitor cycloheximide (40 μM, 30 min) completely prevented the KCl-induced increase in CDKL5 levels (Fig. 1*F*). Complementary, real time PCR was employed to investigate whether membrane depolarization induced *Cdkl5* transcription and/or the induction of well known CREB-responsive immediate early genes, such as *Akt1*, *Egr1*, *Glur2*, and c-*Fos* (Ref. 18 and Fig. 1*G*). A modest but significant increase in *Cdkl5* transcription was observed in neurons treated with KCl; this induction was comparable with that observed for the other

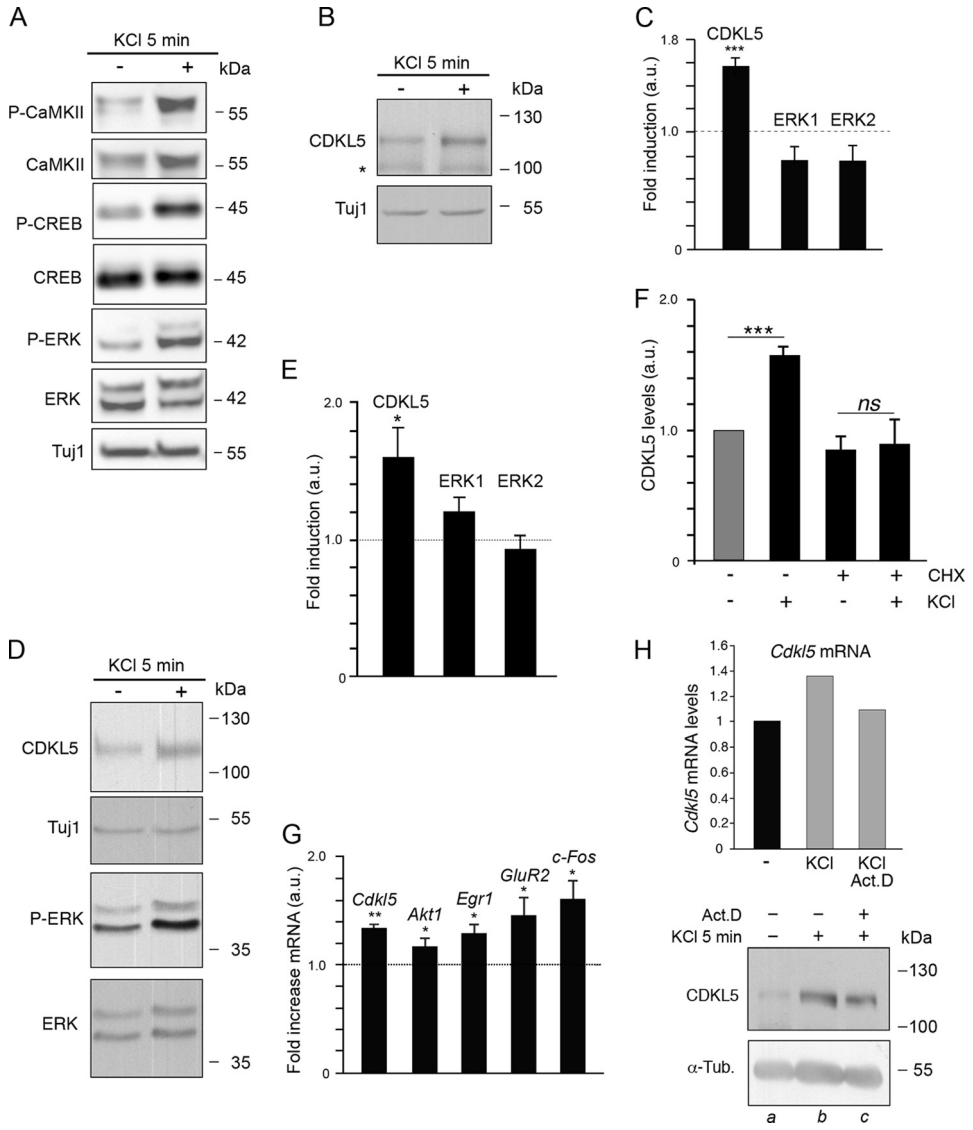

FIGURE 1. **Neuronal depolarization induces CDKL5 expression.** *A*, WB of hippocampal neurons treated at DIV7 with KCl for 5 min. Whole cell lysates were analyzed for phosphorylated and total CaMKII, CREB, and ERKs. Tuj1 was used as loading control. *B*, CDKL5 levels were analyzed in neurons treated as in *A*, using Tuj1 as a loading control. The *asterisk* indicates an unspecific band sometimes occurring with anti-CDKL5 and resistant to three specific shRNAs. *C*, graph showing the fold increase in CDKL5 and ERK1/2 protein levels in depolarized neurons over basal levels indicated with the *dotted line*. *D*, WB showing CDKL5 levels and ERK1/2 phosphorylation in cortical slices (P30–P35) perfused or not with KCl for 5 min. *E*, the graph shows the fold induction of CDKL5 and ERK1/2 protein levels in KCl-treated cortical slices. *F*, graph showing the fold change in CDKL5 levels in neurons treated for 5 min with KCl after 30 min of pretreatment with cycloheximide (*CHX*) as indicated. *G*, graph showing the fold change in mRNA levels of the indicated genes in KCl-treated DIV7 hippocampal neurons with respect to nontreated cells. *H*, CDKL5 levels in neurons treated with actinomycin D (*Act.D*) for 30 min and thereafter with KCl for 5 min as indicated. α-Tubulin was used as internal standard. Graphs in *C* and *E*–*G* represent the means ± S.E. of $n \geq 3$ experiments. *, $p < 0.05$; **, $p < 0.01$; ***, $p < 0.001$.

early responsive genes. When transcription was blocked through actinomycin D treatment (Fig. 1*H*, *upper panel*), the KCl-mediated induction of CDKL5 was nonetheless comparable with that of the control (Fig. 1*H*, *lower panels*, compare *lanes b* and *c* with *lane a*), demonstrating that the activity-dependent CDKL5 increase relies on translation of pre-existing mRNA.

Synaptic Stimulation Induces the Localized Translation of CDKL5 mRNA—The subcellular distribution of CDKL5 in the nuclear and cytoplasmic compartments is modulated by specific stimuli (13); in the dendrites, the protein colocalizes in the postsynaptic compartment with PSD-95 (6, 7). Thus, we employed a biochemical approach to investigate whether the KCl-dependent induction of CDKL5 occurs in the soma or whether, in analogy with other factors involved in synaptic activity, it preferentially occurs in the dendrites (Fig. 3, *A*–*C*). Treated and untreated high density neuronal cultures (DIV16; see "Experimental Procedures" and Ref. 19) were fractionated, and two protein extracts were obtained enriched in cell bodies or dendrites, respectively. The successful fractionation was verified by WB (Fig. 3*A*), which showed the presence of histone H3 or PSD-95 mainly in the somatic or dendritic fractions, respectively. We found that CDKL5 protein levels increase preferentially in the dendritic fraction upon KCl stimulation, whereas its levels remain rather constant in the soma (Fig. 3, *B* and *C*). We hypothesized that *Cdkl5* mRNA might get translated in the

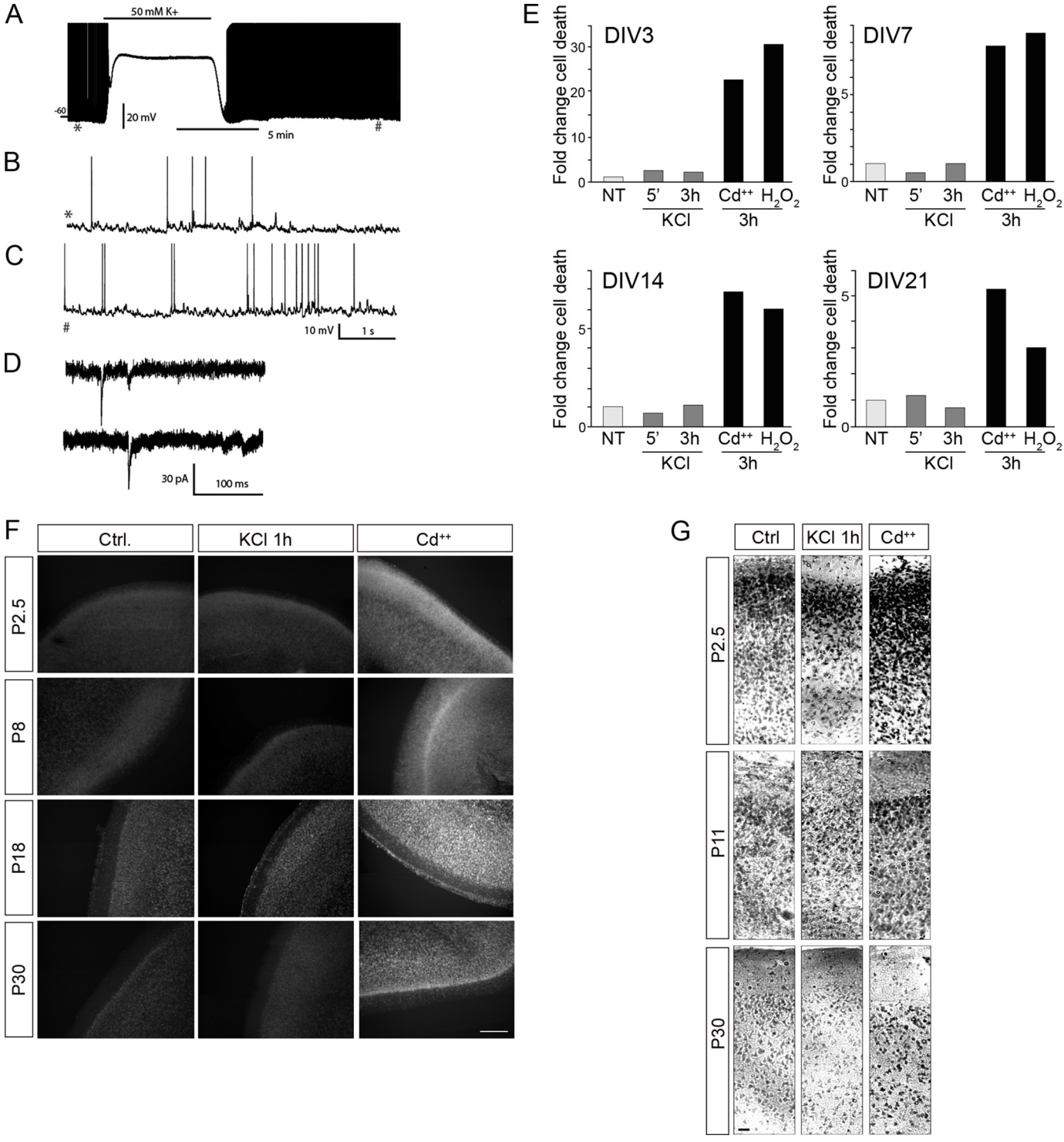

FIGURE 2. **Viability is maintained in hippocampal neurons and cortical slices upon KCl treatment.** *A*, whole cell current clamp recording from a cultured hippocampal neuron (DIV19). Membrane potential (V_m) dynamics is shown before, during, and after application of high KCl (50 mM in physiological saline; equimolar substitution with NaCl) for ~6.5 min (no injected current). Note that during KCl application, the cell depolarizes to −5 mV and spontaneous firing stops presumably because of depolarization block. After washout, firing resumes with no apparent cellular damage (control, ~1.5 Hz; 14 min after washout: ~2.2 Hz). *B* and *C*, two short (6-s) epochs from *A* are shown at higher time resolution. *B*, control (* in *A*); *C*, ~14 min after KCl washout (# in *A*). Note frequent postsynaptic potentials appearing among spikes. In *A–C*, spikes are clipped to 0 mV. *D*, voltage clamp recording from another cell (DIV 15) subjected to 5-min application of 50 mM KCl. *Top trace*, control; *bottom trace*, 23 min after start of KCl washout. Excitatory postsynaptic currents occurring at low frequency are visible in both traces. Similar recordings were obtained in three more cells. *E*, percentage of propidium iodide positive hippocampal neurons at DIV3, 7, 14, and 21 upon treatment with 50 mM KCl for 5 min or 3 h. As control of death induction, neurons were treated with Cd^{2+} (0.5 mM, 3 h) or H_2O_2 (200 μM, 3 h). *F*, propidium iodide staining of cortical slices from P2.5, P8, P18, and P30 mice upon perfusion for 1 h with 3 mM KCl (control) or 30 mM KCl or to induce necrosis with 0.5 mM Cd^{2+} for 3 h. *Scale bar*, 200 μm. *G*, TUNEL assay of cortical slices from P2.5, P11, and P30 mice perfused with 30 mM KCl (1 h) or with 0.5 mM Cd^{2+} (3 h). *Scale bar*, 20 μm. *Ctrl*, control; *NT*, not treated.

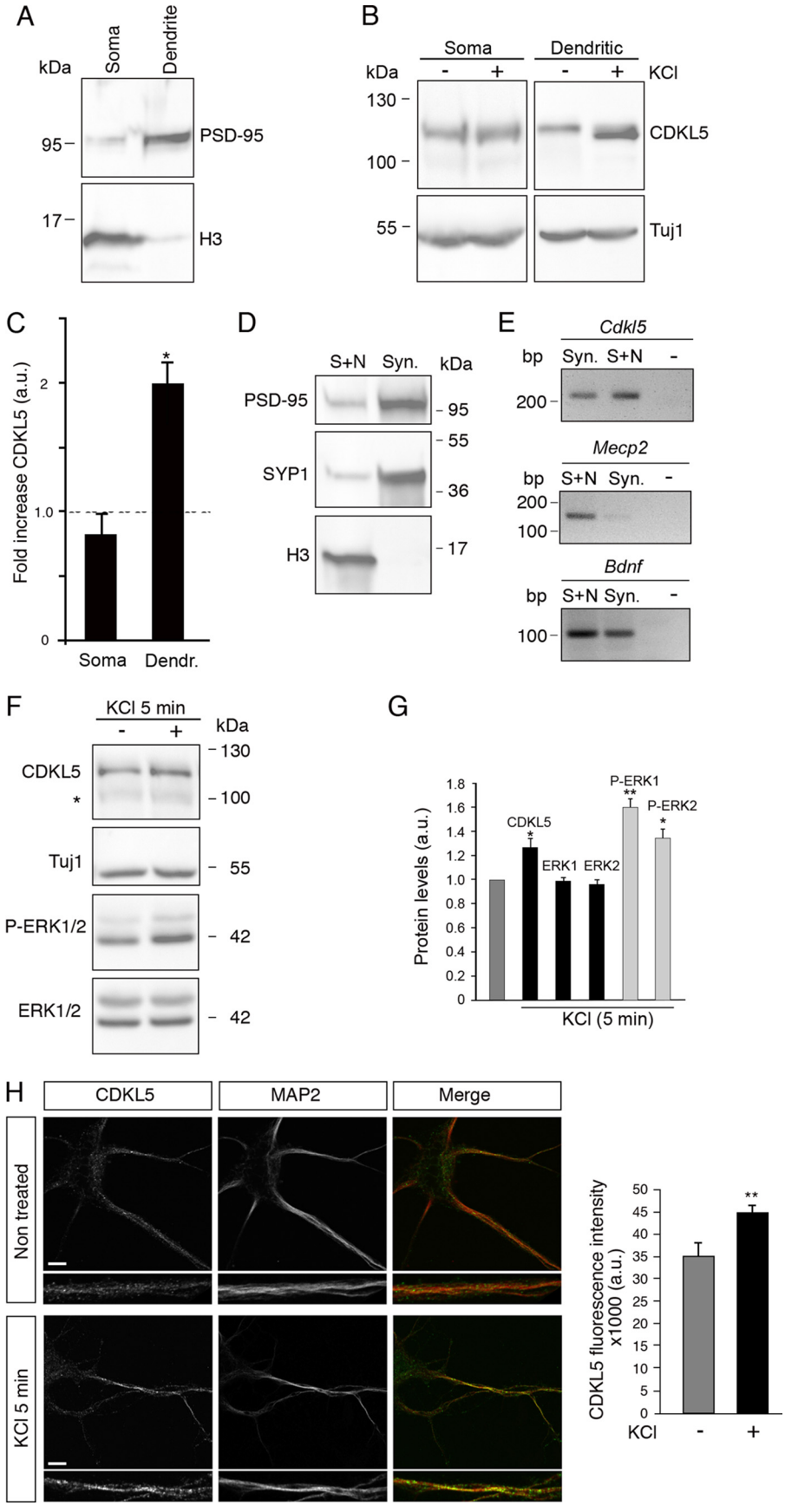
A
Soma
Dendrite
kDa
95
PSD-95
17
H3
B
Soma
Dendritic
kDa
- + - +
KCl
130
100
CDKL5
55
Tuj1
C
Fold increase CDKL5 (a.u.)
2
1.0
0
*
Soma
Dendr.
D
S+N
Syn.
kDa
PSD-95
95
55
SYP1
36
H3
17
E
Cdkl5
bp
Syn.
S+N
-
200
Mecp2
bp
S+N
Syn.
-
200
100
Bdnf
bp
S+N
Syn.
-
100
F
KCl 5 min
- +
kDa
CDKL5
*
130
100
Tuj1
55
P-ERK1/2
42
ERK1/2
42
G
Protein levels (a.u.)
1.8
1.6
1.4
1.2
1.0
0.8
0.6
0.4
0.2
0
CDKL5
*
ERK1
ERK2
P-ERK1
**
P-ERK2
*
KCl (5 min)
H
CDKL5
MAP2
Merge
Non treated
KCl 5 min
CDKL5 fluorescence intensity x1000 (a.u.)
50
45
40
35
30
25
20
15
10
5
0
**
KCl
-
+

neuronal periphery, and we therefore analyzed synaptoneurosomes (see "Experimental Procedures"), which are fractions enriched in isolated functional pre- and postsynaptic terminals, from adult mouse cortices (P30–P35). The enrichment of PSD-95 and synaptophysin (SYP1) in the synaptic extract verified the fractionation, whereas a significant contamination with cell bodies was excluded staining for histone H3 (Fig. 3*D*). By RT-PCR, we revealed the presence of *Cdkl5* mRNA in the synaptoneurosomal fraction together with *Bdnf* transcripts, used as positive control; on the contrary, and as expected, we were unable to reveal the presence of *Mecp2* mRNA in this fraction (Fig. 3*E*). After 5 min of stimulation of synaptoneurosomes with KCl, CDKL5 levels were subtly but significantly increased together with the activation of ERKs, demonstrated by the increased ratio of phosphorylated to total ERKs (Fig. 3, *F* and *G*). Eventually, the dendritic induction of CDKL5 upon depolarization was confirmed also in DIV7 neurons by confocal microscopy using MAP2 as dendritic marker (Fig. 3*H*).

Membrane Depolarization Induces Dephosphorylation of CDKL5 and Its Proteasome-mediated Degradation—Having demonstrated the depolarization-dependent stimulation of CDKL5 synthesis, we studied the time course of the induction and of its maintenance, treating DIV7 neurons with KCl (50 mM) for 0, 5, 20, 40, 60, and 180 min. CDKL5 levels (Fig. 4*A*) rapidly increased but subsequently declined, reaching basal levels within 20 min after stimulation and completely disappearing after 3 h of treatment. This result was confirmed in a complex native neuronal network by comparing CDKL5 levels in young adult (P30–35) cortical slices perfused for 1 h with KCl with those in unstimulated slices (Fig. 4, *B* and *C*). To verify whether a sustained stimulation is required for the down-regulation of CDKL5, we treated DIV7 hippocampal neurons for 5 min with KCl and returned them to basal conditions for 3 or 24 h before WB analysis. As shown in Fig. 4*D*, a short stimulation is sufficient to down-regulate CDKL5. However, protein expression returned to base line levels after 24 h recovery in resting conditions, thus demonstrating that CDKL5 levels are dynamically tuned in response to neuronal activity.

Because we have previously demonstrated that CDKL5 levels can be regulated through proteasomal degradation (13, 20), we tested whether this mechanism is also involved in the observed down-regulation. DIV7 neurons were incubated with the proteasomal inhibitor MG132 (50 μM) prior to KCl induction. Indeed, the presence of MG132 contained CDKL5 reduction after sustained KCl treatment (Fig. 4, *E* and *F*). As already proposed (13), in the presence of MG132, CDKL5 levels rise in unstimulated neurons as well, therefore confirming that CDKL5 turnover is constitutively regulated by proteasomal degradation.

While we were performing these experiments, we noticed that, depending on the electrophoretic conditions, CDKL5 shows an increased mobility upon 20 min KCl induction. Because the migration of some proteins is affected by their phosphorylation status and protein phosphorylation has frequently been associated with neuronal activation and synaptic plasticity, we investigated whether CDKL5 phosphorylation is modulated upon membrane depolarization. As shown in Fig. 5*A*, after 20 min of KCl stimulation and under appropriate electrophoretic conditions (7% SDS-PAGE with 77:1 acrylamide: bis-acrylamide), CDKL5 migrates mainly as a single band with a higher mobility than the prominent band from untreated neurons. We incubated unstimulated or stimulated neuronal extracts with λ-phosphatase and confirmed that the mobility of the dephosphorylated kinase is identical to that caused by prolonged KCl stimulation, therefore confirming that the acquired higher mobility is caused by CDKL5 dephosphorylation (Fig. 5*B*).

We proceeded analyzing whether a brief stimulation was sufficient to induce the appearance of the faster isoform of CDKL5. Neurons were thus depolarized by KCl for 5 min and allowed to recover for another 15 min in resting medium. The brief stimulation was sufficient to induce CDKL5 dephosphorylation that gets more pronounced upon longer incubation in the resting medium (Fig. 5*C*). To reproduce this observation in a more complex neuronal network, we analyzed the electrophoretic mobility of CDKL5 from depolarized cortical slices (Fig. 5*D*). In immature cortices (P6.5), the mobility of CDKL5 is not affected even after a prolonged depolarization (1 h); on the contrary, at P11.5 the same stimulus induces the appearance of small amounts of a faster migrating isoform of CDKL5. At P21 and P30, CDKL5 dephosphorylation is visible after only a 5-min pulse of KCl, therefore suggesting that this modification correlates with neuronal maturation. Accordingly, in undifferentiated neuronal cells, such as mouse Neuro 2a, the mobility of CDKL5 is affected by phosphorylation (Fig. 5*E*), but prolonged KCl treatment induces neither its dephosphorylation nor its degradation (Fig. 5, *F* and *G*). Altogether, these data indicate that only in mature neurons, membrane depolarization is associated with a rapid and transient increase in CDKL5 levels followed by an event of dephosphorylation; further, they suggest that in addition to being rapidly synthesized, CDKL5 gets quickly degraded after neuronal activation.

NMDARs Mediate CDKL5 Induction—As schematized in Fig. 6*A*, neuronal activation can induce local protein synthesis

FIGURE 3. **CDKL5 is synthesized locally at the level of the synapses.** *A*, the purity of somatic and dendritic fractions of cortical neurons (DIV16) was confirmed by WB using histone H3 and PSD-95 as somatic and dendritic markers, respectively. *B*, WB showing CDKL5 levels in somatic and dendritic fractions from KCl-treated neurons (5 min). *C*, graph showing the fold change in CDKL5 levels in the soma and dendrites (*Dendr.*) of KCl-treated neurons over basal levels (*dotted line*). *D*, cortices from P30–P35 brains were fractionated into somatic/nuclear (*S*+*N*) or synaptic fractions (*Syn*); the fractionation quality was confirmed by WB with antibodies against PSD-95, SYP1, and histone H3. *E*, RNA isolated from synaptoneurosomal and somatic/nuclear fractions was reverse transcribed and amplified by PCR using primers against *Cdkl5*, *Mecp2*, and *Bdnf*. Controls with no DNA are indicated as "−." *F*, WB showing CDKL5 levels and ERK1/2 phosphorylation in synaptoneurosomes obtained in *D* and stimulated with KCl for 5 min. *Asterisk* indicates unspecific band. *G*, graph showing the fold change in CDKL5 and ERK protein levels (normalized with Tuj1; *black bars*) and ERK1/2 phosphorylation (normalized with total ERK1/2 level; *light gray bars*) in stimulated synaptoneurosomes compared with untreated samples (*dark gray bar*). *H*, confocal analysis of CDKL5 expression (*green*) in DIV7 neurons treated or not for 5 min with 50 mM KCl. MAP2 (*red*) was used as dendritic marker. The graph shows the quantification of the dendritic CDKL5 fluorescence intensity. *Scale bar*, 10 μm. Graphs in *C* and *G* represent the means ± S.E. of $n \geq 3$ experiments. *, $p < 0.05$; **, $p < 0.01$.

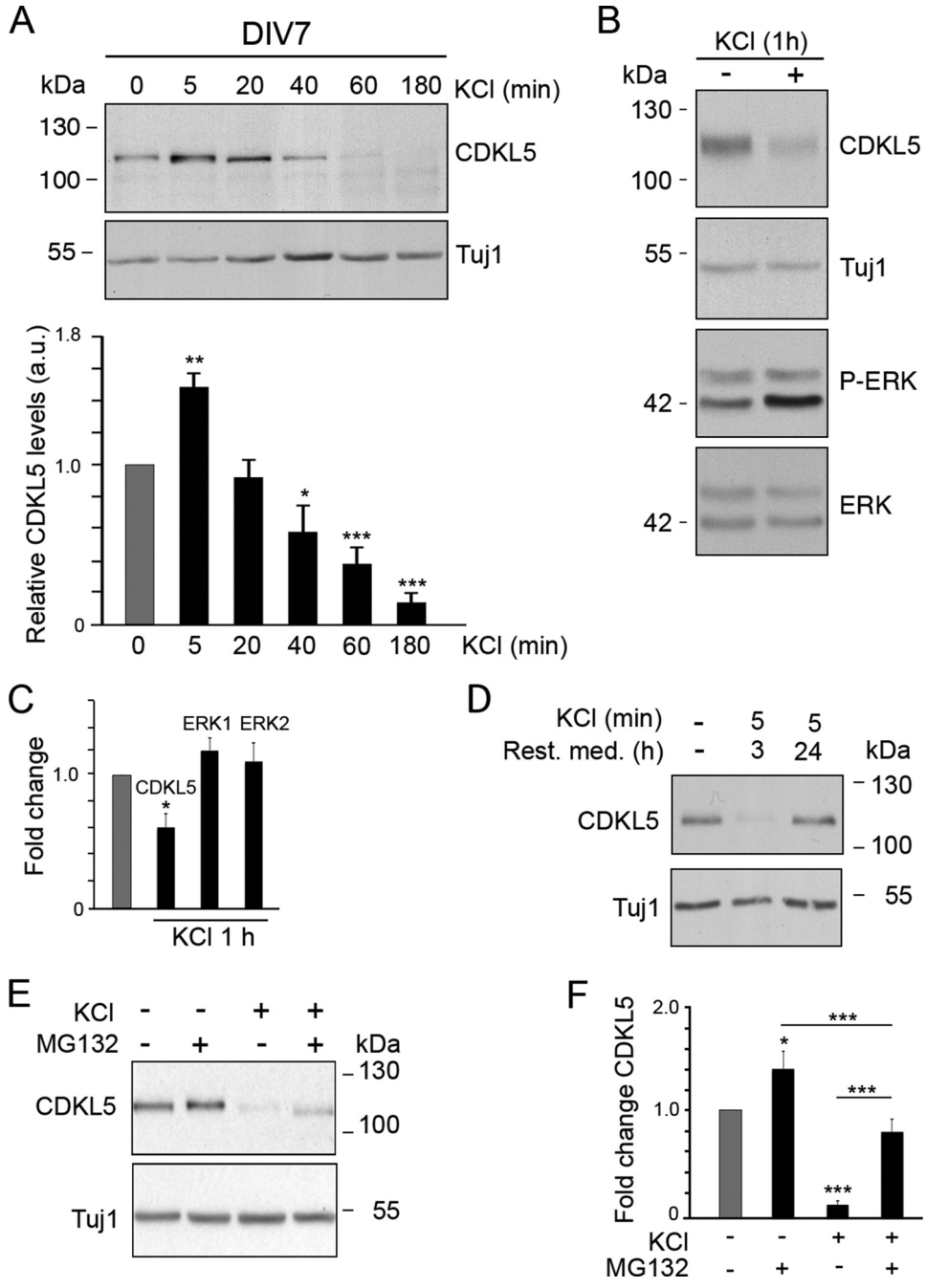

FIGURE 4. **Neuronal depolarization induces proteasome-dependent CDKL5 degradation.** *A*, WB and graph showing CDKL5 levels in DIV7 neurons treated with KCl for the indicated time points. The graph shows the fold change in CDKL5 levels at the different time points of KCl treatment with respect to nontreated neurons (*gray bar*). Tuj1 was used as loading control. The *t* test was performed comparing normalized CDKL5 levels at each time point with those at basal levels. *B*, CDKL5, phosphorylated, and total ERK1/2 levels in cortical slices (P30–P35) after 1 h of perfusion with 30 mM KCl. *C*, graph showing CDKL5 and total ERK1/2 levels in KCl-treated cortical slices compared with the untreated control (*gray bar*). *D*, WB of CDKL5 levels in DIV7 neurons treated with KCl and lysed immediately or upon recovery in the resting medium (*Rest. med.*) for 3 or 24 h. *E*, CDKL5 levels in DIV7 neurons treated for 3 h with KCl, for 6 h with MG132, or with both. *F*, graph showing the fold change in CDKL5 levels in neurons treated as in *E*. *Asterisks* above the *bars* indicate the statistical significance compared with basal levels (*gray bar*). Graphs in *A*, *C*, and *F* represent the means ± S.E. of $n \geq 3$ experiments. *, $p < 0.05$; **, $p < 0.01$; ***, $p < 0.001$.

mainly through NMDARs, AMPARs, or voltage-dependent calcium channels; thus, we proceeded investigating the upstream signals that regulate the activation of CDKL5 protein synthesis upon membrane depolarization. To block KCl-mediated calcium influx, we pretreated hippocampal cultures with EGTA and demonstrated that calcium is required to induce CDKL5 (Fig. 6*B*). This increase was prevented by blocking NMDA or AMPA receptors with the specific antagonists AP5 or CNQX, respectively. It is widely accepted that local protein synthesis requires the activation of ERKs and PKA. Consistently, the KCl-dependent increase in CDKL5 levels was prevented by selectively inhibiting ERKs through preadministration of U0126. Accordingly, we detected an increase in CDKL5 levels, comparable with that of KCl-stimulated neurons, after

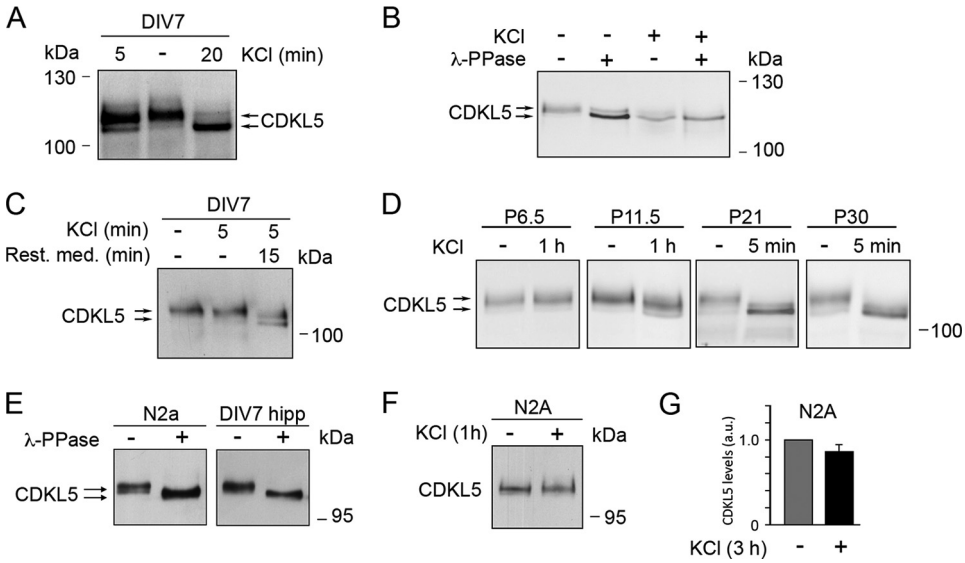

FIGURE 5. **CDKL5 is dephosphorylated upon neuronal depolarization.** *A*, WB showing the mobility of CDKL5 after KCl treatment of hippocampal neurons (DIV7) for 5 or 20 min. *Arrows* indicate slow and fast migrating CDKL5 isoforms. *B*, electrophoretic mobility of CDKL5 in DIV7 hippocampal neurons treated or not with KCl for 20 min and after incubation of the total cell extract with λ-phosphatase (λ-phosphatase) or with the phosphatase buffer alone for 3 h. *C*, migration of CDKL5 in extracts from hippocampal neurons treated for 5 min with KCl and lysed immediately or returned to the resting medium (*Rest. med.*) for 15 min. *D*, mobility of CDKL5 in cortical slices at the indicated postnatal stages perfused with KCl for 1 h or 5 min as indicated. *E*, electrophoretic mobility of CDKL5 in whole cell lysates of mouse N2a cells and hippocampal neurons at DIV7 treated for 3 h with λ-phosphatase or with the buffer alone. *F*, mobility of CDKL5 in extracts of N2a cells treated or not for 1 h with 50 mM KCl. *G*, graph showing CDKL5 levels in N2a cells treated for 3 h with or without 50 mM KCl. No significant change in CDKL5 levels was observed. The graph represents the means ± S.E. of $n = 3$ experiments. In *A–F*, the extracts were separated on 7% gels.

activation of NMDARs by application of NMDA (50 μM for 5 min) or of PKA through forskolin treatment (100 μM for 5 min; Fig. 6*C*). In accordance with the dependence of the ERKs for the activity-dependent induction of CDKL5, the kinase was significantly induced after 5 min of treatment with BDNF that leads to ERK activation through the TrkB receptors (Fig. 6*D*).

Altogether these experiments suggest that a robust Ca^{2+} influx through the NMDA/AMPA receptors induces the observed synaptic synthesis of CDKL5. It is interesting to observe that, in immature neurons (DIV3; see Fig. 8*B*), the KCl-induced expression of CDKL5 is calcium-dependent (data not shown) and maintained in the presence of AP5 and CNQX, therefore suggesting that it does not rely on NMDARs (Fig. 6*E*). Thus, in young neurons, CDKL5 induction appears mediated by voltage-dependent calcium channels (21); to the best of our knowledge, this is the first time that such a switch in the involved intracellular pathways gets proposed.

NMDARs Trigger a PP1-dependent CDKL5 Dephosphorylation Coupled to Its Subsequent Degradation—We then investigated the signals that mediate CDKL5 dephosphorylation in hippocampal neurons. Dephosphorylation was inhibited by preventing extracellular calcium entry, via EGTA, or blocking NMDARs, using AP5; on the contrary, pretreatment of the cultured neurons with CNQX and U0126 did not affect CDKL5 dephosphorylation, indicating that MAP kinases and AMPARs are not involved in the observed phosphate removal (Fig. 7*A*). By incubating hippocampal neurons with NMDA for 20 min, we further demonstrated that Ca^{2+} influx through NMDARs triggers CDKL5 dephosphorylation (Fig. 7*B*). On the contrary, other stimuli such as forskolin or BDNF, which can rapidly induce the expression of CDKL5 (Fig. 6, *C* and *D*), are not able to promote its dephosphorylation (Fig. 7*C*).

Neuronal activation and synaptic plasticity events are mediated by affecting the functions and interactions of a multitude of proteins, mainly through changes in their phosphorylation status; thus, phosphatases, in addition to kinases, play a pivotal role for synaptic plasticity. The majority of these phosphorylation events occur on serine and threonine residues, and in general, the protein phosphatases PP1, PP2A, and calcineurin (PP2B) are considered the most important dephosphorylating enzymes (21). To exclude the involvement of tyrosine dephosphorylation in the KCl-dependent change of CDKL5 electrophoretic mobility, we inhibited tyrosine phosphatases by pretreating primary hippocampal neurons with Na_3VO_4. As clearly shown in Fig. 7*D*, even if tyrosine phosphatases were efficiently inhibited (see "Experimental Procedures"), no inhibition of KCl-dependent CDKL5 dephosphorylation was observed. Hippocampal neurons were then treated with the potent calcineurin inhibitor deltamethrin; as shown in Fig. 7*E*, the drug does not impede CDKL5 dephosphorylation although the efficient inhibition was verified (see "Experimental Procedures"). On the contrary, the faster migrating, dephosphorylated band is not present when 100 nM calyculin A, which inhibits PP1 and PP2A, is administered to neurons, therefore implying the involvement of either or both enzymes (Fig. 7*E*). The presence of 20 nM okadaic acid (OA), which selectively inhibits PP2A and not PP1 (21), does not impede the KCl-dependent CDKL5 dephosphorylation (Fig. 7*F*), suggesting the critical involvement of PP1. Accordingly, 1 μM OA, which inhibits both PP1 and PP2A, impedes the KCl-dependent CDKL5 dephosphorylation, confirming the pivotal involvement of PP1.

Because the prolonged activation of Neuro 2a cells with KCl or of neurons with BDNF induces neither the dephosphory-

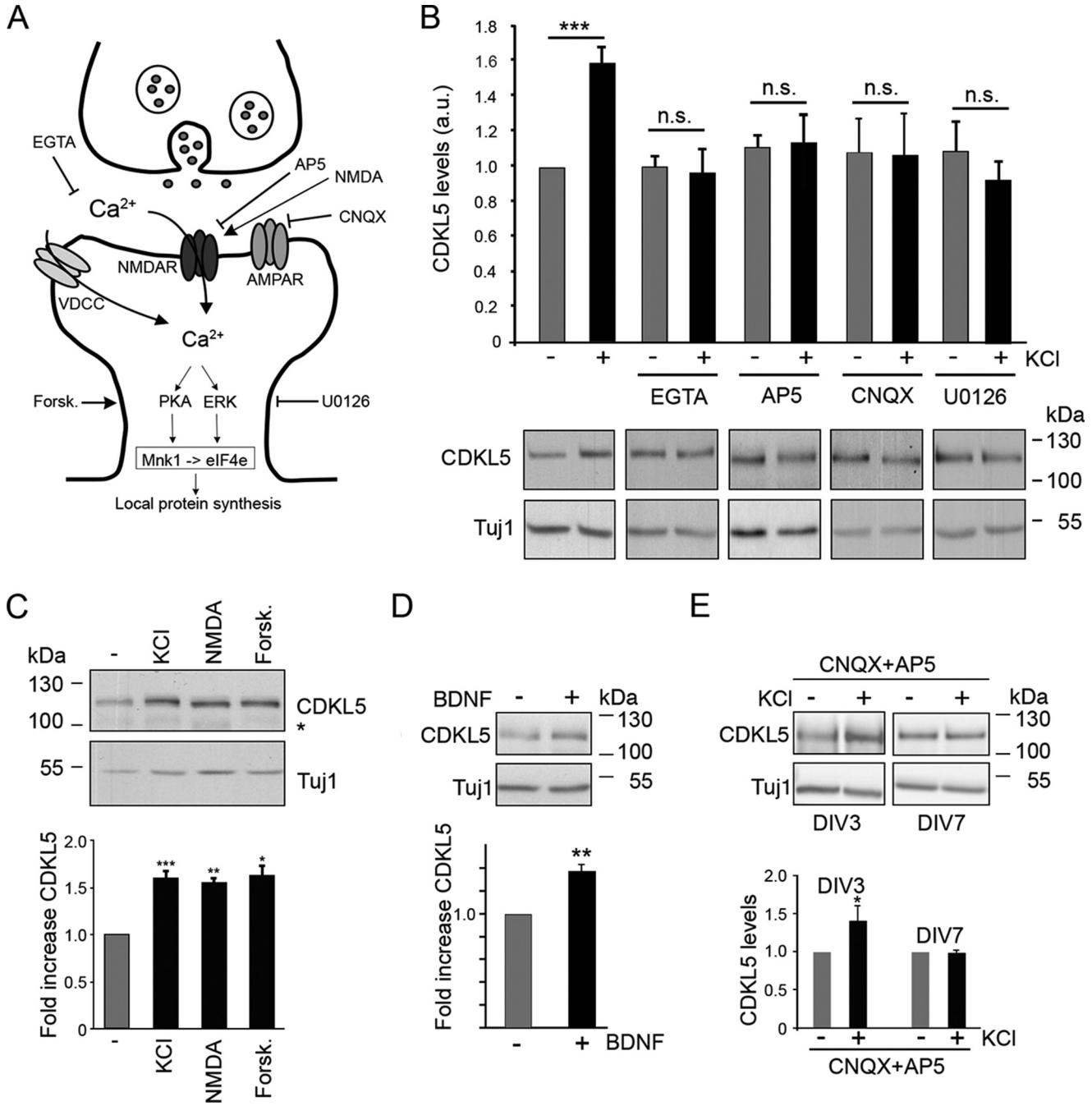

FIGURE 6. **In mature neurons the induction of CDKL5 is mainly mediated by NMDARs.** *A*, schematic illustration of the signaling pathways activated at the synapses and leading to local protein synthesis. *B*, graph and WB showing CDKL5 levels in DIV7 primary hippocampal neurons treated with 50 mM KCl for 5 min alone or upon pretreatment with EGTA, AP5, CNQX, or U0126. Tuj1 was used as internal standard ($n \geq 3$, means ± S.E.). *C* and *D*, WB and graphs showing the fold increase in CDKL5 levels in DIV7 neurons treated for 5 min with KCl, NMDA, or forskolin (*Forsk.*, *C*) and BDNF (*D*) with respect to basal levels. Tuj1 was used as internal standard. *Asterisk* in the WB (*C*) indicates an unspecific band ($n = 4$, means ± S.E.). *E*, CDKL5 levels in neurons at the indicated DIV treated with KCl for 5 min in the presence of both CNQX and AP5 ($n = 6$, means ± S.E.). *, $p < 0.05$; **, $p < 0.01$; ***, $p < 0.001$. *n.s.*, not significant.

lation nor the degradation of CDKL5 (Figs. 5, *F* and *G*, and 7*C*), we suggest the existence of a neuronal-specific molecular link between the activity-dependent dephosphorylation and the degradation of CDKL5 after membrane depolarization. Consequently, we addressed whether dephosphorylation is required for CDKL5 demolition. To this purpose, a prolonged depolarization was applied to DIV7 hippocampal neurons pretreated with MG132, OA, or a combination of both inhibitors, and CDKL5 levels were estimated by Western blotting (Fig. 7*G*). As before, the proteasome inhibition blocked the degradation induced by sustained depolarization (compare *column d* with *column b*); of relevance, under these conditions the faster isoform of CDKL5 gets accumulated (Fig. 7*H*). As shown in *column f* with respect to *column b*, PP1/2A inhibition partially blocks the KCl-induced degradation; in the presence of both inhibitors and KCl (*column h*), CDKL5 levels are rescued without any additional effect (CDKL5 levels in *columns h* and *d* are not statistically different), therefore suggesting that the protea-

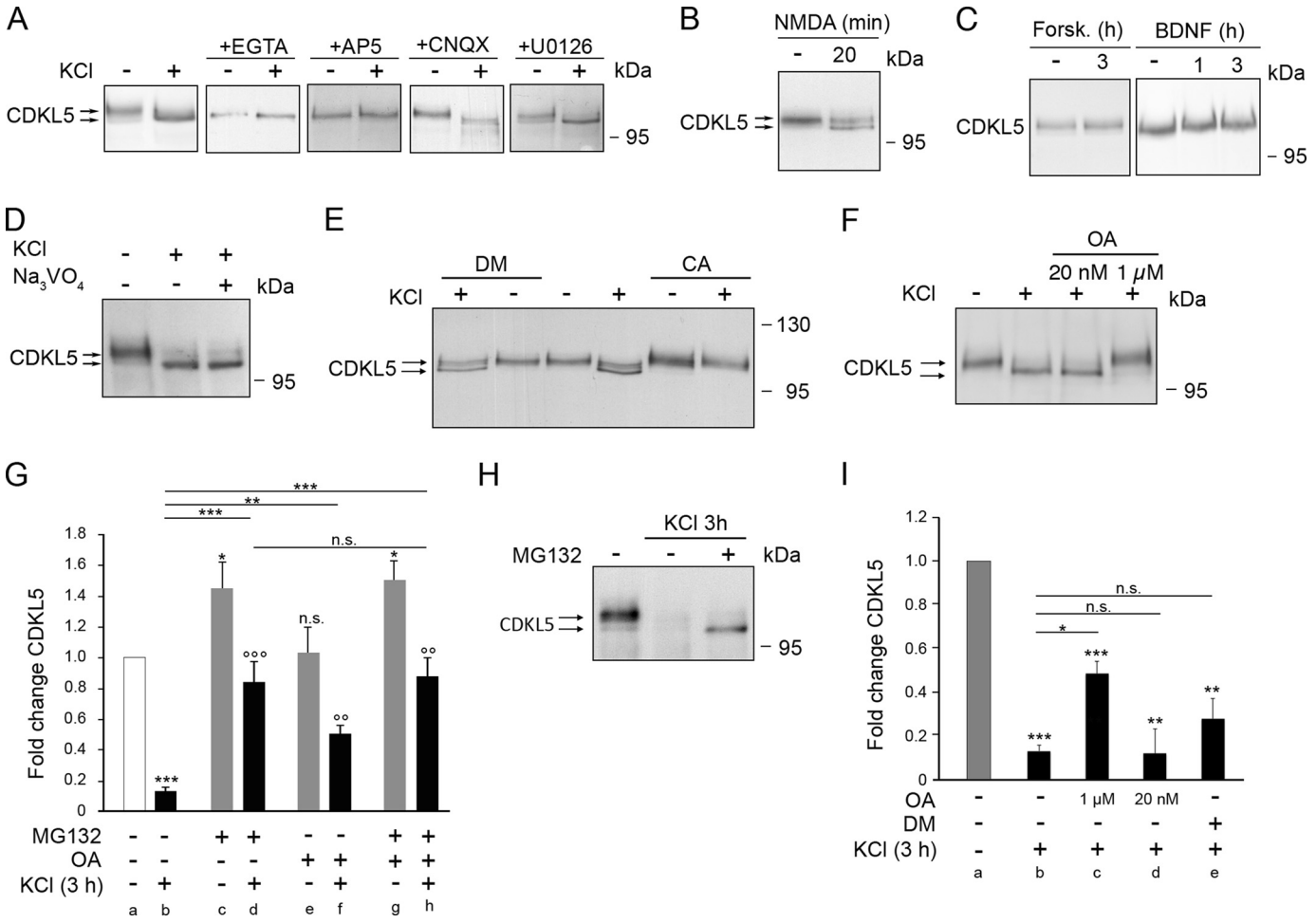

FIGURE 7. **CDKL5 turnover is regulated by its activity-dependent dephosphorylation.** *A*, mobility of CDKL5 in DIV7 neurons treated with KCl (20 min) alone or upon pretreatment as indicated. The *arrows* indicate the fast and slow migrating CDKL5 isoforms. *B* and *C*, mobility of CDKL5 in extracts of neurons treated with NMDA, 20 min (*B*) or with forskolin (*Forsk.*, 3 h) or BDNF (1–3 h; *C*). *D* and *E*, mobility of CDKL5 in neurons pretreated with Na_3VO_4 (*D*), deltamethrin (*DM*), or calyculin (*CA*) (*E*), before 20 min KCl stimulation. *F*, CDKL5 mobility in neurons pretreated with 20 nM or 1 μM OA before 20 min KCl stimulation. *G*, graph showing CDKL5 levels after 3 h of KCl stimulation upon pretreatment with OA (1 μM), MG132 (3 h), or both. Statistical significance is indicated by *asterisks* above the *bars* when CDKL5 levels are compared with basal levels (*white bar*) and by *open circles* when compared with their respective controls (*gray bars*). *H*, CDKL5 migration upon 3 h of KCl treatment of neurons with/without pretreatment with MG132. *I*, graph showing CDKL5 levels in neurons pretreated with OA (1 μM or 20 nM) or deltamethrin, before 3 h of KCl stimulation. Graphs in *G* and *I*, $n \geq 3$, means ± S.E.; *, $p < 0.05$; **, $p < 0.01$; ***, $p < 0.001$. In all panels, the extracts were separated on 7% gels. *n.s.*, not significant.

some and the phosphatase PP1 work in the same pathway. Eventually, by testing CDKL5 levels in depolarized neurons pretreated with deltamethrin or different concentrations of OA (Fig. 7*I*), we demonstrated that only by blocking PP1, the enzyme that causes the appearance of the faster migrating CDKL5 isoform, the kinase degradation was impeded (compare lanes *c* and *b*). Thus, we suggest that CDKL5 dephosphorylation by the phosphatase PP1 is mandatory for its subsequent demolition.

Neuronal Maturation Refines the Mechanisms Controlling CDKL5 Levels—As already mentioned, CDKL5 levels increase in response to neuronal maturation (3, 4); further, the protein activity and its subcellular localization are modulated by neuronal development (13). We thus proceeded investigating whether the observed modulation of CDKL5 levels depends on neuronal maturation (from DIV3 to DIV21; Fig. 8). To this purpose, aware that the maturation state of cultured neurons depends on the growth conditions, we characterized our hippocampal neuronal cultures by costaining for the pre- and postsynaptic markers synapsin 1 and GluR2, respectively (Fig. 8*A*). As expected, with both markers DIV3 neurons do not exhibit dendritic punctae, therefore indicating their immaturity. DIV7 neurons are more progressed in the maturation process but are still lacking a clear punctated postsynaptic pattern. From DIV14, the formation of functional synapses between neurons is proved by the discrete GluR2-positive dendritic punctae juxtaposed to synapsin 1-positive presynaptic dots. As shown in Fig. 8 (*B* and *C*), the extent of CDKL5 induction appears to inversely correlate with neuronal maturation, whereas CDKL5 demolition gets progressively faster. Indeed, in young neurons (DIV3), 5 min of KCl treatment is sufficient to significantly induce CDKL5 expression; however, the degradation is retarded upon prolonged KCl treatment and is not accompanied by the appearance of the faster migrating isoform. On the contrary, a very brief depolarization of DIV21 (*inset* in Fig. 8*C*) permits visualization of the induction of CDKL5 that at 5 min is already masked by the very rapid degradation. Altogether, these data reinforce the observation that CDKL5 dephosphorylation

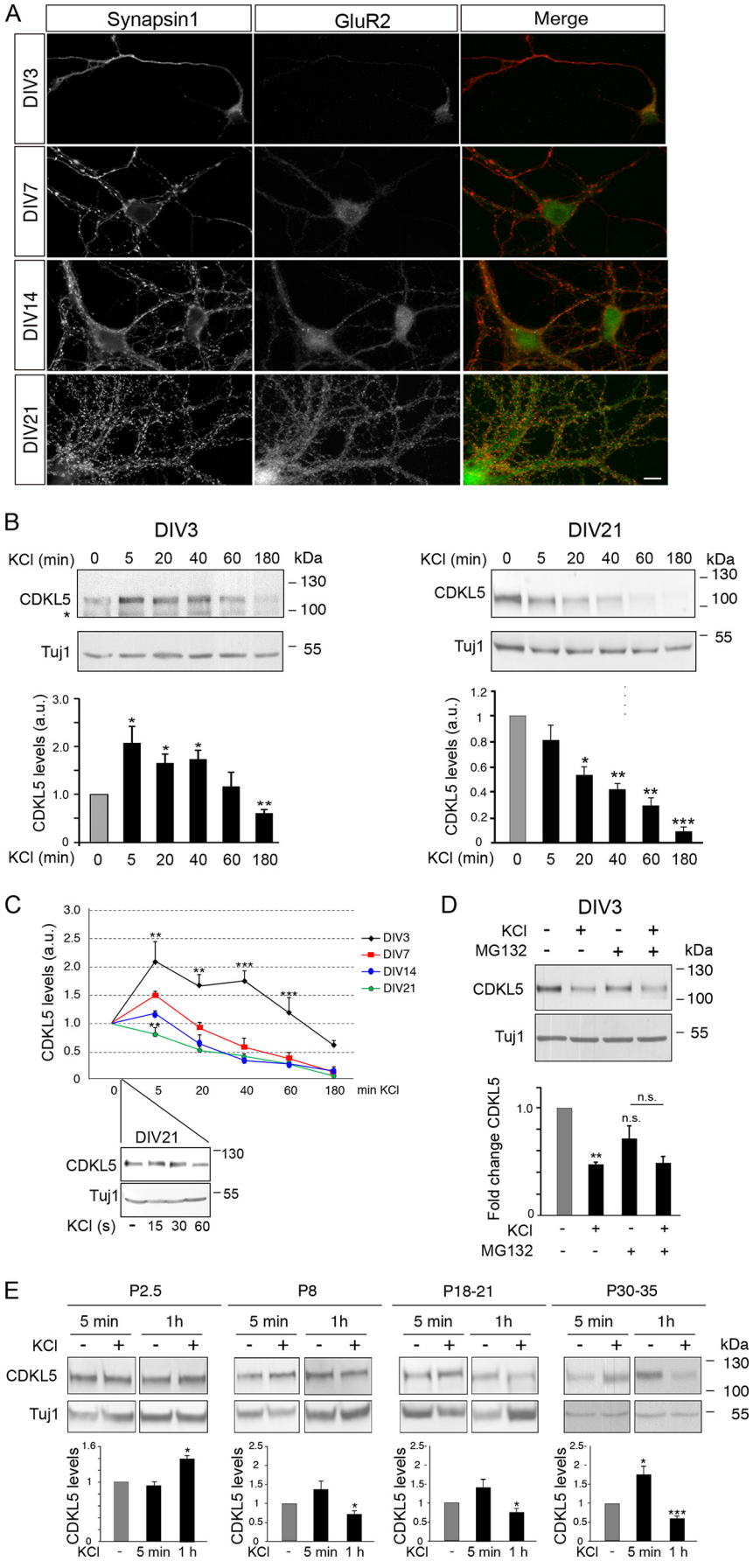
A
Synapsin1
GluR2
Merge
DIV3
DIV7
DIV14
DIV21
B
DIV3
KCl (min) 0 5 20 40 60 180 kDa
CDKL5
Tuj1
130
100
55
CDKL5 levels (a.u.)
DIV21
C
DIV3
DIV7
DIV14
DIV21
min KCl
KCl (s) - 15 30 60
D
KCl
MG132
Fold change CDKL5
n.s.
E
P2.5
P8
P18-21
P30-35
5 min
1h
CDKL5 levels

ensues at a certain maturation stage and suggest that a novel mechanism of control is imposed on CDKL5 upon neuronal maturation, permitting the kinase levels to be more rapidly and finely tuned. Accordingly, as shown in Fig. 8*D*, in immature neurons, CDKL5 levels are only slightly affected by the proteasome system. Interestingly, the differential regulation of CDKL5 at different developmental stages was recapitulated in a more complex *ex vivo* system: a 1-h KCl stimulation is required in newborn mice to induce CDKL5 expression, whereas at further developmental stages, CDKL5 promptly responds to brief KCl stimulation and undergoes degradation if the stimulus is prolonged, with a kinetic resembling that observed in cultured neurons (Fig. 8*E*).

DISCUSSION

In this study, we reveal that neuronal activation and the consequent calcium influx up-regulates CDKL5 levels within 5 min of stimulation. Although *Cdkl5* transcription is induced by membrane depolarization, localized activation of protein synthesis appears as the main mechanism involved in the observed up-regulation. In fact, the kinetics of induction of CDKL5 protein levels is not compatible with its dependence on prior transcription. Moreover, the response occurs predominantly in the dendritic fraction and can be obtained by depolarizing purified synaptoneurosomes. In immature neurons, this induction does not depend on NMDARs, whereas in more mature neurons AMPARs and NMDARs mediate the KCl-dependent increase of CDKL5. In addition, the kinetics of the decline of this activation changes dramatically with neuronal maturation. In fact, in DIV3 neurons CDKL5 levels remain above the basal ones for 1 h after KCl stimulation, whereas at further developmental stages the kinase returns to basal or even lower levels within few minutes (10 min at DIV14; 20–30 min at DIV7). This suggests that CDKL5 levels need to be tightly regulated and that both gain and loss of functions might be detrimental for proper brain development. Accordingly, duplications in *CDKL5* have very recently been identified in patients with neurologic deficits (22). The developmental regulation of the response of CDKL5 to neuronal activation is further supported by the fact that the KCl-mediated depolarization induces the dephosphorylation of CDKL5 only beyond a certain developmental stage. CDKL5 dephosphorylation depends mostly on PP1 activity, occurs in soma and dendrites (data not shown), and is mandatory for its proteasome-dependent degradation. A similar regulation of phosphorylation, occurring only in mature neurons and depending on effectors downstream of NMDARs, has already been described for CREB, a transcription factor that is widely implicated in synaptic plasticity and memory formation (21). Dephosphorylation and subsequent proteasomal degradation is also commonly used for a prompt regulation of protein functions: among others, the levels of the fragile X syndrome-associated protein FMRP are controlled at the synapses through a dephosphorylation-dependent proteasome-mediated degradation (23).

Recently, Ebert and Greenberg (12) have postulated that networks controlling synapse development and functions are of high relevance for the pathogenesis of autism spectrum disorders. We suggest that CDKL5 might belong to these neuronal activity-dependent signaling pathways whose full characterization should help in understanding the molecular basis of autism spectrum disorders and in developing future therapies.

Molecular biology supports this hypothesis. Indeed, a link between CDKL5 and spine development and plasticity has been established demonstrating that the kinase (i) affects neuronal morphogenesis through cytoskeleton rearrangements (4); (ii) is localized at excitatory synapses where it contributes to correct dendritic spine structure and synapse activity (6, 7); (iii) binds the scaffolding protein PSD-95 (7); and (iv) binds amphiphysin 1, a protein involved in synaptic vesicle endocytosis (24).

Neuronal activity triggers changes in the synapse composition, shape, and strength. This can be achieved by inducing the post-translational modification of synaptic molecules, by the localized synthesis of dendritic proteins, and by altering nuclear gene expression. Locally activated CDKL5 might phosphorylate diverse targets therefore affecting spine maturation and plasticity. For instance, upon neuronal activity, AMPA receptors modify their conductivity through a specific CaMKII-dependent event of phosphorylation (25). Interestingly, CaMKII, the most studied kinase involved in the regulation of long-term potentiation (26), is locally synthetized in the postsynaptic compartment after NMDAR induction (27).

Further, distally transported mRNAs are bound by a number of translational inhibitors that impose a repression that has to be removed locally to permit protein synthesis (28). Few kinases have been identified as being locally up-regulated; their enzymatic activity can affect receptor cycling and activation, translation initiation, or elongation or can be relevant to remove RNA binding repressors or to induce splicing. Thus, in the future, it will be highly relevant to reveal the proteome and the phospho-proteome of activated spines devoid of CDKL5. Of relevance, the vast majority of missense pathogenic mutations localize in the catalytic domain of CDKL5, therefore confirming the relevance of its kinase activity for proper brain function (1).

Synaptic stimulation also transmits signals to the nucleus affecting specific transcription programs. So far, few pieces of evidence suggest that CDKL5 has a role in regulating gene

FIGURE 8. **The response of CDKL5 to depolarization depends on neuronal maturation.** *A*, immunofluorescence of hippocampal neurons at the indicated DIV with antibodies against the pre- and postsynaptic markers, synapsin 1 (*red*) or GluR2 (*green*), respectively. *Scale bar*, 100 μm. *B*, WB and graphs showing CDKL5 levels in hippocampal neurons at DIV3 (*left panels*) and DIV21 (*right panels*) after treatment with KCl for the indicated time points. Tuj1 was used as loading control. *Asterisk* in the WB indicates an unspecific band. The statistical significance (*t* test) was tested by comparing CDKL5 levels at each time point with basal levels (*gray bars*). *C*, graph comparing the changes in CDKL5 levels in neurons at DIV3, 7, 14, and 21 treated with KCl as indicated. The expression of CDKL5 at DIV3, 14, and 21 was compared with the expression at DIV7 by using a two-way analysis of variance test (Bonferroni post-tests; $n \geq 3$); no statistical significance could be determined at any time point between DIV7 and DIV14. The WB in the *small inset* shows the change in CDKL5 levels in DIV21 neurons treated with KCl for the indicated time points. *D*, CDKL5 levels in DIV3 hippocampal neurons treated for 3 h with KCl, for 6 h with MG132, or with both. The graph shows the fold change in CDKL5 levels in treated neurons. $n = 3$, means ± S.E. *, $p < 0.05$; **, $p < 0.01$; ***, $p < 0.001$. *E*, WB and graphs showing CDKL5 levels in cortical slices at the indicated ages perfused with KCl for 5 min or 1 h. ($n \geq 3$).

expression such as its capability to interact with the transcriptional repressor MeCP2 (29), the DNA methyl transferase DNMT1 (30), and with the nuclear speckles involved in RNA splicing (31). Considering the soma, we have demonstrated that neuronal activity first induces *Cdkl5* transcription with kinetics similar to those of immediate early genes and then causes CDKL5 dephosphorylation and degradation. These results reinforce the already hypothesized involvement of CDKL5 in influencing gene expression programs indicating the importance of defining the transcriptional signature of activated neurons devoid of CDKL5. Therefore, in the future we will investigate which pathways affect the observed regulation of CDKL5 and its possible involvement in synaptic plasticity, particularly in long-term potentiation and long-term depression.

Acknowledgments—We are indebted to Dr. R. Fesce for valuable suggestions and thank Desirée Zambroni from the ALEMBIC facility for expertise in the microscopy analysis. We thank the Italian parents' associations L'Albero di Greta and ProRett Ricerca for supporting our research.

REFERENCES

1. Kilstrup-Nielsen, C., Rusconi, L., La Montanara, P., Ciceri, D., Bergo, A., Bedogni, F., and Landsberger, N. (2012) What we know and would like to know about CDKL5 and its involvement in epileptic encephalopathy. *Neural. Plast.* **2012,** 728267
2. Bertani, I., Rusconi, L., Bolognese, F., Forlani, G., Conca, B., De Monte, L., Badaracco, G., Landsberger, N., and Kilstrup-Nielsen, C. (2006) Functional consequences of mutations in CDKL5, an X-linked gene involved in infantile spasms and mental retardation. *J. Biol. Chem.* **281,** 32048–32056
3. Rusconi, L., Salvatoni, L., Giudici, L., Bertani, I., Kilstrup-Nielsen, C., Broccoli, V., and Landsberger, N. (2008) CDKL5 expression is modulated during neuronal development and its subcellular distribution is tightly regulated by the C-terminal tail. *J. Biol. Chem.* **283,** 30101–30111
4. Chen, Q., Zhu, Y. C., Yu, J., Miao, S., Zheng, J., Xu, L., Zhou, Y., Li, D., Zhang, C., Tao, J., and Xiong, Z. Q. (2010) CDKL5, a protein associated with Rett syndrome, regulates neuronal morphogenesis via Rac1 signaling. *J. Neurosci.* **30,** 12777–12786
5. Carouge, D., Host, L., Aunis, D., Zwiller, J., and Anglard, P. (2010) CDKL5 is a brain MeCP2 target gene regulated by DNA methylation. *Neurobiol. Dis.* **38,** 414–424
6. Ricciardi, S., Ungaro, F., Hambrock, M., Rademacher, N., Stefanelli, G., Brambilla, D., Sessa, A., Magagnotti, C., Bachi, A., Giarda, E., Verpelli, C., Kilstrup-Nielsen, C., Sala, C., Kalscheuer, V. M., and Broccoli, V. (2012) CDKL5 ensures excitatory synapse stability by reinforcing NGL-PSD95 interaction in the postsynaptic compartment and is impaired in patient iPSC derived neurons. *Nat. Cell Biol.* **14,** 911–923
7. Zhu, Y. C., Li, D., Wang, L., Lu, B., Zheng, J., Zhao, S. L., Zeng, R., and Xiong, Z. Q. (2013) Palmitoylation-dependent CDKL5-PSD-95 interaction regulates synaptic targeting of CDKL5 and dendritic development. *Proc. Natl. Acad. Sci. U.S.A.* **110,** 9118–9123
8. Wang, I. T., Allen, M., Goffin, D., Zhu, X., Fairless, A. H., Brodkin, E. S., Siegel, S. J., Marsh, E. D., Blendy, J. A., and Zhou, Z. (2012) Loss of CDKL5 disrupts kinome profile and event-related potentials leading to autistic-like phenotypes in mice. *Proc. Natl. Acad. Sci. U.S.A.* **109,** 21516–21521
9. Amendola, E., Zhan, Y., Mattucci, C., Castroflorio, E., Calcagno, E., Fuchs, C., Lonetti, G., Silingardi, D., Vyssotski, A. L., Farley, D., Ciani, E., Pizzorusso, T., Giustetto, M., and Gross, C. T. (2014) Mapping pathological phenotypes in a mouse model of CDKL5 disorder. *PLoS One* **9,** e91613
10. Ricciardi, S., Boggio, E. M., Grosso, S., Lonetti, G., Forlani, G., Stefanelli, G., Calcagno, E., Morello, N., Landsberger, N., Biffo, S., Pizzorusso, T., Giustetto, M., and Broccoli, V. (2011) Reduced AKT/mTOR signaling and protein synthesis dysregulation in a Rett syndrome animal model. *Hum. Mol. Genet.* **20,** 1182–1196
11. Flavell, S. W., and Greenberg, M. E. (2008) Signaling mechanisms linking neuronal activity to gene expression and plasticity of the nervous system. *Annu. Rev. Neurosci.* **31,** 563–590
12. Ebert, D. H., and Greenberg, M. E. (2013) Activity-dependent neuronal signalling and autism spectrum disorder. *Nature* **493,** 327–337
13. Rusconi, L., Kilstrup-Nielsen, C., and Landsberger, N. (2011) Extrasynaptic *N*-methyl-D-aspartate (NMDA) receptor stimulation induces cytoplasmic translocation of the CDKL5 kinase and its proteasomal degradation. *J. Biol. Chem.* **286,** 36550–36558
14. Lombardi, G., Leonardi, P., and Moroni, F. (1996) Metabotropic glutamate receptors, transmitter output and fatty acids: studies in rat brain slices. *Br. J. Pharmacol.* **117,** 189–195
15. De Rubeis, S., Pasciuto, E., Li, K. W., Fernández, E., Di Marino, D., Buzzi, A., Ostroff, L. E., Klann, E., Zwartkruis, F. J., Komiyama, N. H., Grant, S. G., Poujol, C., Choquet, D., Achsel, T., Posthuma, D., Smit, A. B., and Bagni, C. (2013) CYFIP1 coordinates mRNA translation and cytoskeleton remodeling to ensure proper dendritic spine formation. *Neuron* **79,** 1169–1182
16. Chen, W. G., Chang, Q., Lin, Y., Meissner, A., West, A. E., Griffith, E. C., Jaenisch, R., and Greenberg, M. E. (2003) Depression of BDNF transcription involves calcium-dependent phosphorylation of MeCP2. *Science* **302,** 885–889
17. Zhou, Z., Hong, E. J., Cohen, S., Zhao, W. N., Ho, H. Y., Schmidt, L., Chen, W. G., Lin, Y., Savner, E., Griffith, E. C., Hu, L., Steen, J. A., Weitz, C. J., and Greenberg, M. E. (2006) Brain-specific phosphorylation of MeCP2 regulates activity dependent Bdnf transcription, dendritic growth, and spine maturation. *Neuron* **52,** 255–269
18. Okuno, H. (2011) Regulation and function of immediate early genes in the brain: beyond neuronal activity markers. *Neurosci. Res.* **69,** 175–186
19. Verpelli, C., Piccoli, G., Zibetti, C., Zanchi, A., Gardoni, F., Huang, K., Brambilla, D., Di Luca, M., Battaglioli, E., and Sala, C. (2010) Synaptic activity controls dendritic spine morphology by modulating eEF2-dependent BDNF synthesis. *J. Neurosci.* **30,** 5830–5842
20. Williamson, S. L., Giudici, L., Kilstrup-Nielsen, C., Gold, W., Pelka, G. J., Tam, P. P., Grimm, A., Prodi, D., Landsberger, N., and Christodoulou, J. (2012) A novel transcript of cyclin-dependent kinase-like 5 (CDKL5) has an alternative C-terminus and is the predominant transcript in brain. *Hum. Genet.* **131,** 187–200
21. Sala, C., Rudolph-Correia, S., and Sheng, M. (2000) Developmentally regulated NMDA receptor-dependent dephosphorylation of cAMP response element-binding protein (CREB) in hippocampal neurons. *J. Neurosci.* **20,** 3529–3536
22. Szafranski, P., Golla, S., Jin, W., Fang, P., Hixson, P., Matalon, R., Kinney, D., Bock, H. G., Craigen, W., Smith, J. L., Bi, W., Patel, A., Wai Cheung, S., Bacino, C. A., and Stankiewicz, P. (2014) Neurodevelopmental and neurobehavioral characteristics in males and females with CDKL5 duplications. *Eur. J. Hum Genet.* 10.1038/ejhg. 2014.217
23. Nalavadi, V. C., Muddashetty, R. S., Gross, C., and Bassell, G. J. (2012) Dephosphorylation-induced ubiquitination and degradation of FMRP in dendrites: a role in immediate early mGluR-stimulated translation. *J. Neurosci.* **32,** 2582–2587
24. Sekiguchi, M., Katayama, S., Hatano, N., Shigeri, Y., Sueyoshi, N., and Kameshita, I. (2013) Identification of amphiphysin 1 as an endogenous substrate for CDKL5, a protein kinase associated with X-linked neurodevelopmental disorder. *Arch. Biochem. Biophys.* **535,** 257–267
25. Hardingham, G. E., Arnold, F. J., and Bading, H. (2001) A calcium microdomain near NMDA receptors: on switch for ERK-dependent synapse-to-nucleus communication. *Nature Neurosci.* **4,** 565–566
26. Lisman, J., Yasuda, R., and Raghavachari, S. (2012) Mechanisms of CaMKII action in Long Term Potentiation. *Nat. Rev. Neurosci.* **13,** 169–182
27. Scheetz, A. J., Nairn, A. C., and Constantine-Paton, M. (2000) NMDA receptor-mediated control of protein synthesis at developing synapses. *Nat. Neurosci.* **3,** 211–216
28. Gkogkas, C., Sonenberg, N., and Costa-Mattioli, M. (2010) Translational control mechanism in long-lasting synaptic plasticity and memory. *J. Biol. Chem.* **285,** 31913–31917
29. Mari, F., Azimonti, S., Bertani, I., Bolognese, F., Colombo, E., Caselli, R., Scala, E., Longo, I., Grosso, S., Pescucci, C., Ariani, F., Hayek, G., Balestri,

P., Bergo, A., Badaracco, G., Zappella, M., Broccoli, V., Renieri, A., Kilstrup-Nielsen, C., and Landsberger, N. (2005) CDKL5 belongs to the same molecular pathway of MeCP2 and it is responsible for the early-onset seizure variant of Rett syndrome. *Hum. Mol. Genet.* **14,** 1935–1946

30. Kameshita, I., Sekiguchi, M., Hamasaki, D., Sugiyama, Y., Hatano, N., Suetake, I., Tajima, S., and Sueyoshi, N. (2008) Cyclin-dependent kinase-like 5 binds and phosphorylates DNA methyltransferase 1. *Biochem. Biophys. Res. Commun.* **377,** 1162–1167
31. Ricciardi, S., Kilstrup-Nielsen, C., Bienvenu, T., Jacquette, A., Landsberger, N., and Broccoli, V. (2009) CDKL5 influences RNA splicing activity by its association to the nuclear speckle molecular machinery. *Hum. Mol. Genet.* **18,** 4590 – 4602